
STRUCTURE, PHASE TRANSFORMATIONS, AND DIFFUSION

On the Prediction of Stacking Fault Energy on Medium Mn Steels

H. Essoussi^{a, b, *}, S. Ettaqi^b, and E. Essadiqi^b

^a *Laboratory of Materials, Metallurgy and Process Engineering, ENSAM, Meknes, Morocco*

^b *Université Internationale de Rabat (UIR), Aerospace Engineering School, Rabat Salé, Morocco*

*e-mail: hamza.essoussi1@gmail.com

Received September 3, 2020; revised December 18, 2020; accepted December 23, 2020

Abstract—Stacking fault energy estimation is considered as an important stage in the process of designing advanced high-strength steels. Therefore, in the present study, the thermochemical model of Olsen and Cohen was employed to calculate the stacking fault energy (SFE) in Fe–C–Mn–Al–Si steels with <0.6 wt % C, manganese 3–10 wt %, aluminum 0.5–3 wt % and silicon 0.5–3 wt %. The calculation findings revealed that besides the importance of high Mn, the addition of Al and Si leads to SFE values in the range of 20–40 mJ/m² that allows the activation of twinning induced plasticity (TWIP) and/or transformation induced plasticity (TRIP) effects.

Keywords: stacking fault energy, medium Mn steels, retained austenite

DOI: 10.1134/S0031918X21140076

INTRODUCTION

Recently, Medium Mn steels have been considered as promising candidates for automobile structural components due to their excellent mechanical properties [1–7]. However, these good properties depend mainly on the volume fraction, stability, and stacking fault energy of the retained austenite. By taking in first consideration the effect of stacking fault energy, during deformation of these materials, the strengthening may be due to the deformation-induced martensitic transformation (TRIP) [1], and/or mechanical twinning (TWIP) [8]. Especially the transformation-induced plasticity occurs in steels with SFEs < 20 mJ/m² the deformation twinning has been observed in steels with sfes between 20 and 40 mJ/m². In the case of high SFE (>40 mJ/m²) dislocations are rarely dissociated, thus, the deformation process is controlled mainly by dislocation glide [9, 10]. Therefore, temperature and chemical composition of the alloy can affect strongly the occurrence and the extend of these deformation mechanisms.

The detailed knowledge on the precise effect of the alloying elements on the SFE are complex and need to be investigated closely in each case in order to be fully understood. Many previous studies found in the literature focused on the investigation of the correlation between SFE and chemical composition influence, by using transmission electron microscopy (TEM) [11], and X-ray diffraction [12], while others estimated the SFE by empirical relationships [13].

Within this context, the present study aims to contribute to the prediction of the SFE of Fe–Mn–Al–

C–Si steels via a thermodynamic model of Olsen and Cohen with improved parameters and analyze the effects of temperature and alloying elements especially Al and Si in three different manganese concentrations [7–10–13] wt % and 0.2 wt % of carbon.

1. THERMODYNAMIC MODEL OF THE SFE

It is well known that there are two types of stacking fault energies defined in the literature, the so-called intrinsic stacking fault energy which is the sequence ABCACABC..., this type consists of two planes of hexagonal close packed structure (hcp). However, the second type is the extrinsic SF or twin SF which has a stacking sequence of ABCACBCAB..., this extrinsic type appears as if an additional C layer has been inserted in the fcc lattice, which produces a twin with the stacking sequence ACB. The extrinsic SF is created by the passage of single Shockley partials on two consecutive planes and its effect on the overall SFE is too small in comparison to the intrinsic SFE [14]. As well, because of the most common stacking fault in a fcc crystal, is the intrinsic type and the negligible contribution of the extrinsic term, Only the intrinsic SF is considered for the energy calculation using the thermodynamics-based approach. Therefore according to the thermodynamic model proposed by Olsen and Cohen [15], it can be seen that the SFE includes both volume and surface energy contributions which are in agreement with the classical nucleation theory. The SFE of such a fault may be expressed in terms of the molar Gibbs energy difference between the

Table 1. Functions describing the change in Gibbs energies

Parameter	Function	Ref.
$\Delta G_{\text{Fe}}^{\gamma \rightarrow \epsilon}$	$-2243.38 + 4.309T$ (J/mol)	[27]
$\Delta G_{\text{Mn}}^{\gamma \rightarrow \epsilon}$	$-1000 + 1.123T$ (J/mol)	[27]
$\Delta G_{\text{Al}}^{\gamma \rightarrow \epsilon}$	558.85 (J/mol)	[22]
$\Delta G_{\text{C}}^{\gamma \rightarrow \epsilon}$	-22166 (J/mol)	[28, 29]
$\Delta G_{\text{Si}}^{\gamma \rightarrow \epsilon}$	$-560 - 8T$ (J/mol)	[30]
$\Delta G_{\text{FeC}}^{\gamma \rightarrow \epsilon}$	42500 (J/mol)	[16]
$\Delta G_{\text{FeAl}}^{\gamma \rightarrow \epsilon}$	3328 (J/mol)	[22]
$\Delta G_{\text{FeMn}}^{\gamma \rightarrow \epsilon}$	$2873 - 717(X_{\text{Fe}} - X_{\text{Mn}})$ (J/mol)	[17]
$\Delta G_{\text{FeSi}}^{\gamma \rightarrow \epsilon}$	$2850 + 3520(X_{\text{Fe}} - X_{\text{Si}})$ (J/mol)	[30]
$\Delta G_{\text{MnC}}^{\gamma \rightarrow \epsilon}$	26910 (J/mol)	[28, 29]
$\Delta G_{\text{MnSi}}^{\gamma \rightarrow \epsilon}$	1780 (J/mol)	[29]
$\Delta G_{\text{FeMnX/C}}^{\gamma \rightarrow \epsilon}$	$a = 1246$ J/mol; $b = 24.29$ J/mol; $c = -17.175$ J/mol	[30]

nucleus of the hcp phase and the fcc phase of the matrix $\Delta G^{\gamma \rightarrow \epsilon}$, and a interface energy σ [16, 17]. This approach has later been extensively used in the literature for calculating the SFE in austenitic stainless steels [18, 19], Fe–C–Mn alloys [20], high manganese austenitic steels (TWIP steels), [22–24] and shape memory alloys.

Within this approach, the intrinsic SFE per unit area γ_{SFE} is expressed as:

$$\gamma_{\text{SFE}} = 2\rho\Delta G^{\gamma \rightarrow \epsilon} + 2\sigma, \quad (1)$$

where ρ is the molar surface density in a close packed plane in moles per unit area which is related to the lattice parameter a of the fcc phase, as follows:

$$\rho = \frac{4}{\sqrt{3}} \frac{1}{a^2 N_A}, \quad (2)$$

$\Delta G^{\gamma \rightarrow \epsilon}$ is the molar Gibbs free energy of transformation $\gamma \rightarrow \epsilon$, σ is the energy per surface unit of a {111} interface between γ and ϵ . The molar Gibbs free energy can be divided into chemical and magnetic contributions as follow:

$$\Delta G^{\gamma \rightarrow \epsilon} = \Delta G_{\text{chem}}^{\gamma \rightarrow \epsilon} + \Delta G_{\text{mag}}^{\gamma \rightarrow \epsilon}. \quad (3)$$

In its turn the chemical contribution is divided into two terms:

$$\Delta G_{\text{chem}}^{\gamma \rightarrow \epsilon} = \Delta G_{\text{FeMnX}}^{\gamma \rightarrow \epsilon} + \Delta G_{\text{FeMnX/C}}^{\gamma \rightarrow \epsilon}. \quad (4)$$

According the regular and subregular solution model [16], the $\Delta G_{\text{FeMnX}}^{\gamma \rightarrow \epsilon}$ that is defined as the Gibbs

energy due to the chemical contribution of all substitution elements in the fcc lattice can be expressed as:

$$\Delta G_{\text{FeMnX}}^{\gamma \rightarrow \epsilon} = \sum_i x_i \Delta G_i^{\gamma \rightarrow \epsilon} + x_{\text{Fe}} x_{\text{Mn}} \Delta G_{\text{FeMn}}^{\gamma \rightarrow \epsilon} + x_{\text{Fe}} x_{\text{Si}} \Delta G_{\text{FeSi}}^{\gamma \rightarrow \epsilon}, \quad (5)$$

where $\Delta G_i^{\gamma \rightarrow \epsilon}$ is the Gibbs energy of the chemical contribution of the element i ($i = \text{Fe}, \text{Mn}, \text{Al}$ and Si) with the molar fraction x_i . The data used are mainly taken from literature, the detail expressions, values and functions are summed up in Table 1.

Moreover, carbon as a main interstitial element in the alloy system has an important effect as a disturbance of the former fcc solid solution, as well its effect depends on the manganese addition [16]. Thus, the empirical law describing this carbon effect is:

$$\Delta G_{\text{FeMnX/C}}^{\gamma \rightarrow \epsilon} = \frac{a}{x_c} (1 - e^{-bx_c}) + cx_{\text{Mn}}. \quad (6)$$

On the other hand the magnetic contribution is defined as follow:

$$\Delta G_{\text{mag}}^{\gamma \rightarrow \epsilon} = G_{\text{m}}^{\epsilon} - G_{\text{m}}^{\gamma}, \quad (7)$$

where

$$G_{\text{m}}^j = f\left(\frac{T}{T_{\text{N}}^j}\right) RT \ln\left(1 + \frac{\beta^j}{\mu_{\text{B}}}\right), \quad (8)$$

$$j = \gamma, \epsilon.$$

With β^j and T_{N}^j present respectively, the magnetic moment and Néel temperature of phase j [16], μ_{B} is the Bohr magneton, and f is a polynomial function [25] which its expression depends on the phase and Néel temperature:

$$f\left(\frac{T}{T_{\text{N}}^j}\right) = 1 - \left(\frac{1}{D}\right) \times \left(\left(\frac{79\tau^{-1}}{140P} \right) + \frac{474}{497} \left(\frac{1}{P} - 1 \right) \left(\frac{\tau^3}{6} + \frac{\tau^9}{135} + \frac{\tau^{15}}{600} \right) \right). \quad (9)$$

When $\tau \leq 1$

$$f\left(\frac{T}{T_{\text{N}}^j}\right) = -\left(\frac{1}{D}\right) \left(\left(\frac{\tau^{-5}}{10} + \frac{\tau^{-15}}{315} + \frac{\tau^{-25}}{1500} \right) \right). \quad (10)$$

When $\tau > 1$

with $P = 0.28$, $D = 2.34$ and $(\tau = T/T_{\text{N}}^j)$.

In addition, the Néel temperature of γ and ϵ expressed en Kelvin depends on the chemical composition as can be seen form their expression:

$$T_{\text{N}}^{\gamma} = 669.27(1 - \exp(-5.46X_{\text{Mn}})) - 0.241X_{\text{C}}(1 - X_{\text{Mn}} - X_{\text{C}}) - 109,$$

$$T_{\text{N}}^{\epsilon} = 580X_{\text{Mn}}$$

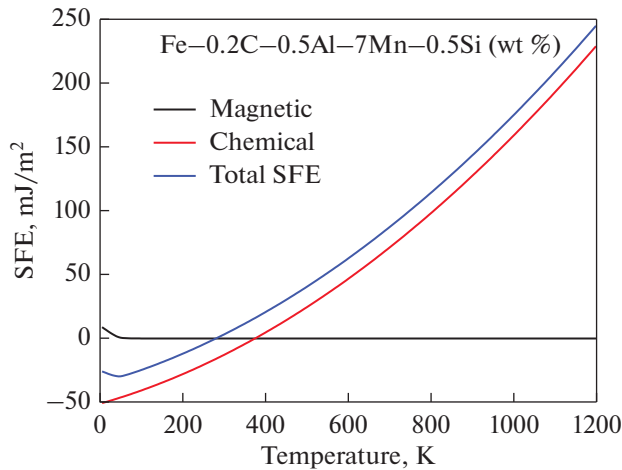


Fig. 1. Calculated evolution of the SFE versus temperature for the Fe-0.2C-7Mn-0.5Al-0.5Si (wt %) alloy.

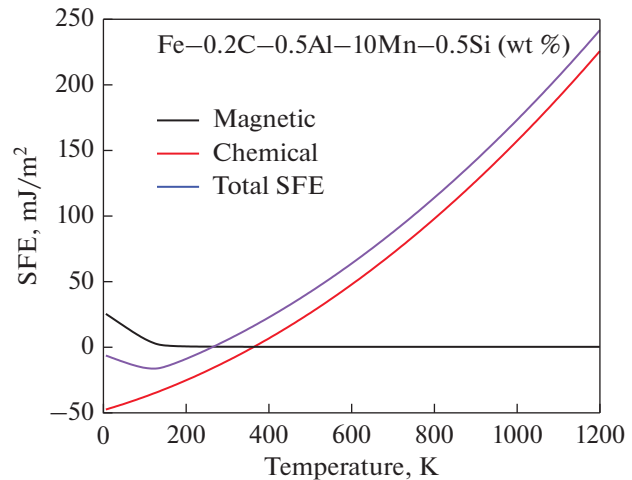


Fig. 2. Calculated evolution of the SFE versus temperature for the Fe-0.2C-10Mn-0.5Al-0.5Si (wt %) alloy.

the term of surface energy has been used as a fitting parameter by many authors to get the results of the calculated SFE that fit with the experimental values. Indeed, S.M. Cotes et al. [26] using measurements of extended dislocation nodes found an interfacial energy values ranging from 16 to 26 mJ/m² (ref), Akbari et al. [24] have used an interfacial energy of 15 mJ/m², while Dumay et al. [16] utilized $\sigma = 8$ mJ/m², therefore, in our case the value of $\sigma = 8$ mJ/m² is taken in all performed calculations.

2. RESULTS AND DISCUSSION

For comparison purpose the global effects of temperature and alloying elements on the SFE in three different Fe-C-Mn-Al-Si are shown in this section. Indeed, There are many reports in the literature about the effect of carbon additions on the SFE, thus depending on the other alloying elements the SFE of the austenite grains could increase [31], or decrease [32] with a carbon content for this reason the 0.2 wt % C is fixed for all alloys to only highlight the effect of the other alloy elements. Therefore, for three Fe-0.2% C-Mn-based alloys with the minimum additions of Al and Si, the SFE values and both chemical and magnetic contributions versus temperature are plotted in Figs. 1–3 for Mn content of 7, 10 and 13 wt %, respectively.

It can be seen from Figs. 1–3 that there is a decrease in SFE with increasing of temperature until around 50 to 200°C depending on the Mn content then, it increases with increasing temperature, this trend was reported by Remy et al. [33] through TEM observations and found that the nodes of dislocation decrease with temperature, which explain the SFE increase with temperature. However, Hickel et al. [34] found an opposite effect based on the TEM characterization and ab initio calculations. On the other hand,

from Fig. 4, it is important to point out that the change of the SFE with manganese and temperature is stronger at a very low temperature than that observed at high temperature such results are consistent with the results obtained by Lee et al. [35] on Fe-Mn binary system. The same tendency was found by Dai et al. for austenitic steels [36]. Moreover, it can be seen that the SFE of the three systems is in the range that leads to martensitic transformation.

According to Suh et al. [37], Al and Si additions are needed in the medium Mn steels for many reasons, one among them is to increase the SFE of the steel, thus the effects of Al and Si additions in the above three Fe-C-Mn systems were compared as shown respectively in Figs. 5 and 6.

From Figs. 5 and 6, it is worth to notice, that the effects of Al and Si become more important when the

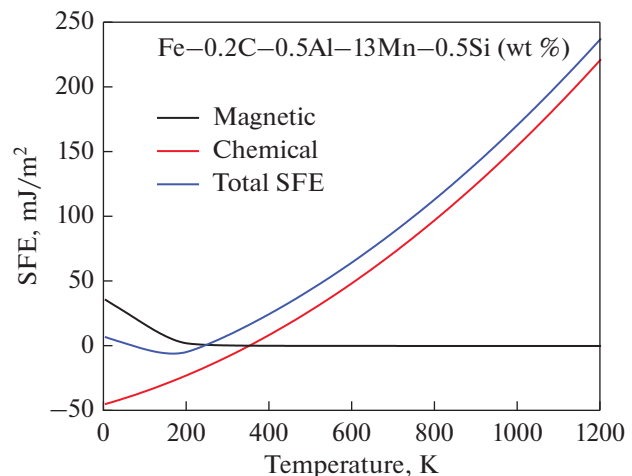


Fig. 3. Calculated evolution of the SFE versus temperature for the Fe-0.2C-13Mn-0.5Al-0.5Si (wt %) alloy.

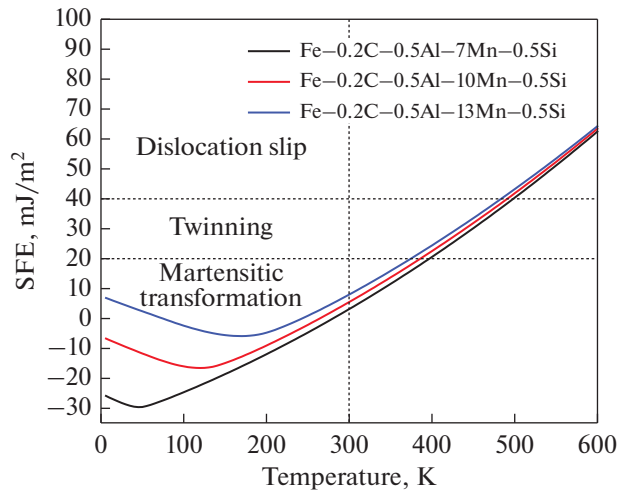


Fig. 4. Calculated evolution of the SFE versus temperature for the three alloys with low Al and Si additions.

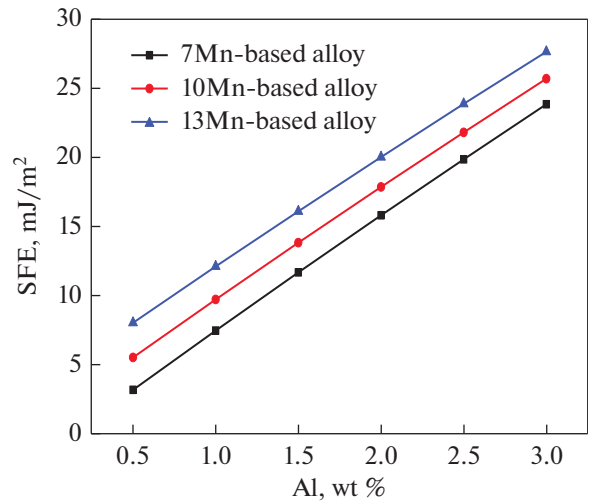


Fig. 5. Calculated evolution of the SFE versus Al additions for three alloys.

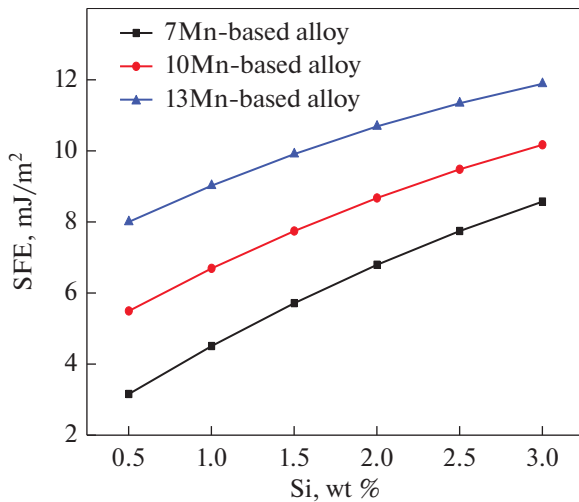


Fig. 6. Calculated evolution of the SFE versus Si additions for three alloys.

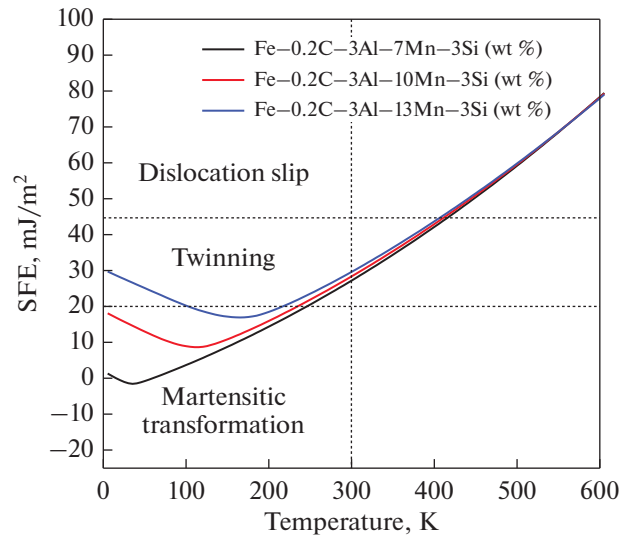


Fig. 7. Calculated evolution of the SFE versus temperature for the three alloys with high Al and Si additions.

Mn content is increased. While, it can be seen from Fig. 7 that at room temperature the SFE value of the three alloys with higher Al and Si contents gives rise to mechanical twinning instead of martensitic transformation observed in the case of the same alloys with low Al and Si contents as shown in Fig. 3.

3. CONCLUSIONS

This paper highlighted the effect of temperature, and alloy elements (Mn Si Al) on the SFE in the Medium Mn steels characterized by composition that consist of Fe–Mn–Al–C–Si, the results support the following conclusions:

- The present model shows a good capacity to reflect the effect of temperature and chemical composition on the SFE of medium Mn steels.
- Al and Si addition have the strongest influences when the Mn content is increased, then we have established that the Mn addition is the key element responsible for the SFE value.
- Increases in the Al and Si favored the twinning by increasing the SFE.
- The estimation of SFE to predict the deformation mechanism becomes an important step in the alloy design of medium Mn steels.

REFERENCES

1. D. W. Suh, H. Ryu, M. S. Joo, H. S. Yang, K. Lee, and H. K. D. H. Bhadeshia, "Medium-alloy manganese-rich transformation-induced plasticity steels," *Metall. Mater. Trans. A* **44**, 286–293 (2013). <https://doi.org/10.1007/s11661-012-1402-3>
2. J. Chen, M. Lv, S. Tang, Z. Liu, and G. Wang, "Correlation between mechanical properties and retained austenite characteristics in a low-carbon medium manganese alloyed steel plate," *Mater. Charact.* **106**, 108–111 (2015). <https://doi.org/10.1016/j.matchar.2015.05.026>
3. G. Mishra, A. K. Chandan, and S. Kundu, "Hot rolled and cold rolled medium manganese steel: Mechanical properties and microstructure," *Mater. Sci. Eng., A* **701**, 319–327 (2017). <https://doi.org/10.1016/j.msea.2017.06.088>
4. W. Q. Cao, C. Wang, J. Shi, M. Q. Wang, W. J. Hui, and H. Dong, "Microstructure and mechanical properties of Fe–0.2C–5Mn steel processed by ART-annealing," *Mater. Sci. Eng., A* **528** (22–23), 6661–6666 (2011). <https://doi.org/10.1016/j.msea.2011.05.039>
5. R. Rana and S. B. Singh, *Automotive Steels: Design, Metallurgy, Processing and Applications* (Elsevier, Amsterdam, 2016).
6. B. Hu, H. Luo, F. Yang, and H. Dong, "Recent progress in medium-Mn steels made with new designing strategies, a review," *J. Mater. Sci. Technol.* **33** (12), 1457–1464 (2017). <https://doi.org/10.1016/J.JMST.2017.06.017>
7. H. Aydin, I. H. Jung, E. Essadiqi, and S. Yue, "Twinning and tripping in 10% Mn steels," *Mater. Sci. Eng., A* **591**, 90–96 (2014). <https://doi.org/10.1016/j.msea.2013.10.088>
8. B. B. He, H. W. Luo, and M. X. Huang, "Experimental investigation on a novel medium Mn steel combining transformation-induced plasticity and twinning-induced plasticity effects," *Int. J. Plast.* **78**, 173–186 (2016). <https://doi.org/10.1016/j.ijplas.2015.11.004>
9. H. Essoussi, S. Ettaqi, and E. Essadiqi, "The effect of alloying elements on the stacking fault energy of a TWIP steel," *Procedia Manuf.* **22**, 129–134 (2018). <https://doi.org/10.1016/J.PROMFG.2018.03.020>
10. D. T. Pierce, J. A. Jiménez, J. Bentley, D. Raabe, C. Oskay, and J. E. Wittig, "The influence of manganese content on the stacking fault and austenite/ ϵ -martensite interfacial energies in Fe–Mn–(Al–Si) steels investigated by experiment and theory," *Acta Mater.* **68**, 238–253 (2014). <https://doi.org/10.1016/j.actamat.2014.01.001>
11. J. Kim and B. C. De Cooman, "On the stacking fault energy of Fe–18 pct Mn–0.6 pct C–1.5 pct Al twinning-induced plasticity steel," *Metall. Mater. Trans. A* **42** (4), 932–936 (2011). <https://doi.org/10.1007/s11661-011-0610-6>
12. N. I. Medvedeva, M. S. Park, D. C. van Aken, and J. E. Medvedeva, "First-principles study of Mn, Al and C distribution and their effect on stacking fault energies in fcc Fe," *J. Alloys Compd.* **582**, 475–482 (2014). <https://doi.org/10.1016/j.jallcom.2013.08.089>
13. O. A. Zambrano, "Stacking fault energy maps of Fe–Mn–Al–C–Si steels: effect of temperature, grain size, and variations in compositions," *J. Eng. Mater. Technol.* **138** (4), 041010 (2016). <https://doi.org/10.1115/1.4033632>
14. R. Abbaschian, L. Abbaschian, and R. E. Reed-Hill, *Physical Metallurgy Principles* (Cengage Learning, Stamford, CT, 2009).
15. G. B. Olson and M. Cohen, "A general mechanism of martensitic nucleation: Part III. Kinetics of martensitic nucleation," *Metall. Trans. A* **7** (11), 1915–1923 (1976). <https://doi.org/10.1007/BF02654989>
16. A. Dumay, J. P. Chateau, S. Allain, S. Migot, and O. Bouaziz, "Influence of addition elements on the stacking-fault energy and mechanical properties of an austenitic Fe–Mn–C steel," *Mater. Sci. Eng., A* **483–484** (1–2), 184–187 (2008). <https://doi.org/10.1016/j.msea.2006.12.170>
17. S. Allain, J. P. Chateau, O. Bouaziz, S. Migot, and N. Guelton, "Correlations between the calculated stacking fault energy and the plasticity mechanisms in Fe–Mn–C alloys," *Mater. Sci. Eng., A* **387–389** (1–2), 158–162 (2004). <https://doi.org/10.1016/j.msea.2004.01.059>
18. S. Curtze, V. T. Kuokkala, A. Oikari, J. Talonen, and H. Hänninen, "Thermodynamic modeling of the stacking fault energy of austenitic steels," *Acta Mater.* **59** (3), 1068–1076 (2011). <https://doi.org/10.1016/j.actamat.2010.10.037>
19. P. J. Ferreira and P. Müllner, "A thermodynamic model for the stacking-fault energy," *Acta Mater.* **46** (13), 4479–4484 (1998). [https://doi.org/10.1016/S1359-6454\(98\)00155-4](https://doi.org/10.1016/S1359-6454(98)00155-4)
20. J. Nakano and P. J. Jacques, "Effects of the thermodynamic parameters of the hcp phase on the stacking fault energy calculations in the Fe–Mn and Fe–Mn–C systems," *CALPHAD: Comput. Coupling Phase Diagrams Thermochem.* **34** (2), 167–175 (2010). <https://doi.org/10.1016/j.calphad.2010.02.001>
21. Y. K. Lee and C. S. Choi, "Driving force for $\gamma \rightarrow \epsilon$ martensitic transformation and stacking fault energy of γ in Fe–Mn binary system," *Metall. Mater. Trans. A* **31** (2), 355–360 (2000). <https://doi.org/10.1007/s11661-000-0271-3>
22. W. S. Yang and C. M. Wan, "The influence of aluminum content to the stacking fault energy in Fe–Mn–Al–C alloy system," *J. Mater. Sci.* **25** (3), 1821–1823 (1990). <https://doi.org/10.1007/BF01045392>
23. R. Xiong, H. Peng, S. Wang, H. Si, and Y. Wen, "Effect of stacking fault energy on work hardening behaviors in Fe–Mn–Si–C high manganese steels by varying silicon and carbon contents," *Mater. Des.* **85**, 707–714 (2015). <https://doi.org/10.1016/j.matdes.2015.07.072>
24. A. Saeed-Akbari, J. Imlau, U. Prahl, and W. Bleck, "Derivation and variation in composition-dependent stacking fault energy maps based on subregular solution model in high-manganese steels," *Metall. Mater. Trans. A* **40** (13), 3076–3090 (2009). <https://doi.org/10.1007/s11661-009-0050-8>

25. L. Li and T. Y. Hsu, "Gibbs free energy evaluation of the fcc(γ) and HCP(ϵ) phases in Fe–Mn–Si alloys," *CALPHAD: Comput. Coupling Phase Diagrams Thermochem.* **21** (3), 443–448 (1997).
[https://doi.org/10.1016/S0364-5916\(97\)00044-8](https://doi.org/10.1016/S0364-5916(97)00044-8)
26. S. M. Cotes, A. Fernández Guillermet, and M. Sade, "Fcc/Hcp martensitic transformation in the Fe–Mn system: Part II. Driving force and thermodynamics of the nucleation process," *Metall. Mater. Trans. A* **35** (1), 83–91 (2004).
<https://doi.org/10.1007/s11661-004-0111-y>
27. M. Gilliland, "The value added by machine learning approaches in forecasting," *Int. J. Forecast.* **36**, 161–166 (2020).
28. S. Curtze, V. T. Kuokkala, A. Oikari, J. Talonen, and H. Hänninen, "Thermodynamic modeling of the stacking fault energy of austenitic steels," *Acta Mater.* **59** (3), 1068–1076 (2011).
<https://doi.org/10.1016/j.actamat.2010.10.037>
29. S. Allain, J. P. Chateau, O. Bouaziz, S. Migot, and N. Guelton, "Correlations between the calculated stacking fault energy and the plasticity mechanisms in Fe–Mn–C alloys," *Mater. Sci. Eng., A* **387–389** (1–2), 158–162 (2004).
<https://doi.org/10.1016/j.msea.2004.01.059>
30. A. Dumay, J. P. Chateau, S. Allain, S. Migot, and O. Bouaziz, "Influence of addition elements on the stacking-fault energy and mechanical properties of an austenitic Fe–Mn–C steel," *Mater. Sci. Eng., A* **483–484** (1–2), 184–187 (2008).
<https://doi.org/10.1016/j.msea.2006.12.170>
31. W. J. Dan, F. Liu, and W. G. Zhang, "Strain hardening behavior of TWIP steel in plastic deformation with temperature," *Modell. Simul. Mater. Sci. Eng.* **23** (2), 025011 (2015).
<https://doi.org/10.1088/0965-0393/23/2/025011>
32. P. J. Brofman and G. S. Ansell, "On the effect of carbon on the stacking fault energy of austenitic stainless steels," *Metall. Trans. A* **9** (6), 879–880 (1978).
<https://doi.org/10.1007/BF02649799>
33. L. Rémy, A. Pineau, and B. Thomas, "Temperature dependence of stacking fault energy in close-packed metals and alloys," *Mater. Sci. Eng.* **36** (1), 47–63 (1978).
[https://doi.org/10.1016/0025-5416\(78\)90194-5](https://doi.org/10.1016/0025-5416(78)90194-5)
34. T. Hickel et al., "Impact of nanodiffusion on the stacking fault energy in high-strength steels," *Acta Mater.* **75**, 147–155 (2014).
<https://doi.org/10.1016/j.actamat.2014.04.062>
35. Y. K. Lee and C. S. Choi, "Driving force for $\gamma \rightarrow \epsilon$ martensitic transformation and stacking fault energy of γ in Fe–Mn binary system," *Metall. Mater. Trans. A* **31** (2), 355–360 (2000).
<https://doi.org/10.1007/s11661-000-0271-3>
36. Q.-X. Dai, A.-D. Wang, X.-N. Cheng, and X.-M. Luo, "Stacking fault energy of cryogenic austenitic steels," *Chinese Phys.* **11** (6), 596 (2002).
<https://doi.org/10.1088/1009-1963/11/6/315>
37. D.-W. Suh and S.-J. Kim, "Medium Mn transformation-induced plasticity steels: Recent progress and challenges," *Scr. Mater.* **126**, 63–67 (2017).
<https://doi.org/10.1016/J.SCRIPTAMAT.2016.07.013>